Applied Thermal Engineering 217 (2022) 119197

Contents lists available at ScienceDirect

Applied Thermal Engineering

journal homepage: www.elsevier.com/locate/apthermeng

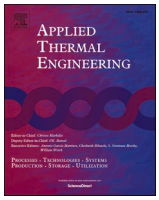

Research Paper

Simulation of gasketed-plate heat exchangers using a generalized model with variable physical properties

André L.M. Nahes [a], Miguel J. Bagajewicz [b,c], André L.H. Costa [a,*]

[a] Rio de Janeiro State University (UERJ), Rua São Francisco Xavier, 524, Maracanã, CEP 20550-900, Rio de Janeiro, RJ, Brazil
[b] Federal University of Rio de Janeiro (UFRJ), Escola de Química, CT, Bloco E, Ilha do Fundão, CEP 21949-900, Rio de Janeiro, RJ, Brazil
[c] School of Chemical, Biological and Materials Engineering, University of Oklahoma, Norman, OK 73019, USA

A B S T R A C T

In this article, we present a new generalized model for the steady-state simulation of gasketed-plate exchangers handling single-phase fluids with properties varying with temperature. The model is based on differential balance equations that are discretized using a finite-difference scheme. The set of equations of the proposed model can simulate gasketed-plate heat exchangers with any configuration, encompassing any number of passes for each stream and including the variation of the streams' physical properties with temperature. The selection of a given configuration is provided by a set of model parameters, without the need to modify the system of equations. Comparisons of the simulation results with closed-form relations valid for an infinite number of plates and with a numerical solution indicate average differences equal to 0.17 % and 0.075 %, respectively. The comparison with experimental data available in the literature indicates mean deviations smaller than 2 °C. The analysis of the simulation results of a typical heat exchanger shows that the models usually employed in the design optimization problems, based on uniform physical properties, may present large departures from the results of our detailed modeling, based on varying properties with temperature, which for its nature is considered more accurate. Moreover, when used in a design, we show that uniform physical properties may yield exchangers that are either oversized or undersized as compared to the use of our model. Therefore, the capacity of the proposed model to provide more accurate simulation results for any gasketed-plate heat exchanger configuration using a unique set of equations is an important contribution to future works involving heat exchanger design optimization.

1. Introduction

Many important industrial plants, such as dairy and beverages employ gasketed-plate exchangers intensively [31,2]. They are also used as an alternative to shell-and-tube exchangers in chemical process plants for some duties. They are more compact and usually have lower capital costs, higher film coefficients, and less propensity to fouling. Their main limitations are related to the presence of gaskets and large pressure drops. Their operating ranges are temperatures below 160 °C – 250 °C and pressure up to 25–30 bar. They are also not suitable for gas–gas applications or highly viscous fluids [18]. Reviews of the performance of gasketed-plate heat exchangers can be found in Elmaaty et al. [8] and Kumar et al. [21].

The conventional modeling approach for gasketed-plate heat exchangers employs the logarithmic mean temperature difference (LMTD) or the effectiveness (ε-NTU) methods. These methods are widely discussed in heat transfer equipment textbooks [31,18,2] and, despite their simplifications, they are still used in several applications, such as the design optimization of gasketed-plate heat exchangers. For example, the ε-NTU method was employed to solve design optimization problems by Hajabdollahi et al. [12], Imran et al. [14], and Raja et al. [29]; the LMTD method was employed in optimization problems by Zhu and Zhang [37], Guo-Yan et al. [9], Picón-Núñez et al. [26], and Xu et al. [36].

The LMTD or ε-NTU methods are based on analytical solutions that assume uniformity of the values of the heat transfer coefficients along the heat transfer surface, ignoring the variation of the physical properties with temperature. Aiming at reducing the error associated with this assumption, these methods adopt the evaluation of the heat transfer coefficients using average temperatures to calculate the corresponding physical properties or average properties of the corresponding values at the end temperatures. The hypothesis of uniform values of the physical properties can provide results with satisfactory accuracy in many cases, but there are several problems where large variations of the physical properties with temperature may bring relevant deviations. Another limitation of the analytical solutions is associated with the effect of the end plates, especially in small heat exchangers. Indeed, the typical expressions of the correction factor of the LMTD or the ε-NTU expressions are based on asymptotic solutions [19]. An attempt to include end effects was performed by Polley and Abu-Khader [27]. These thermal models are also employed using hydraulic modeling based on analytical expressions; specifically using the Darcy–Weisbach equation with hydraulic diameters and uniform values of the physical properties.

To avoid the limitations of analytical solutions, several authors

* Corresponding author.
E-mail address: andrehc@uerj.br (A.L.H. Costa).

https://doi.org/10.1016/j.applthermaleng.2022.119197
Received 18 April 2022; Received in revised form 16 July 2022; Accepted 19 August 2022
Available online 24 August 2022

Nomenclature

b	Mean channel spacing (m)
Cp_n	Heat capacity of the stream that flows in a channel n (J/(kg·K))
Cpc	Heat capacity of the cold stream (J/(kg·K))
Cph	Heat capacity of the hot stream (J/(kg·K))
D_{hyd}	Hydraulic diameter (m)
Dp	Port diameter (m)
f	Friction factor
G	Mass flux in the channel (kg/(m^2·s))
Gp	Mass flux through the port (kg/(m^2·s))
h	Convective heat transfer coefficient (W/(m^2·K))
k	Stream thermal conductivity (W/(m·K))
kw	Thermal conductivity of the plate material (W/(m·K))
Lp	Projected plate length (m)
Lv	Vertical port distance (m)
Lw	Plate width inside gasket (m)
mc_n	Mass flow rate in the channel (kg/s)
mc	Mass flow rates of the cold stream (kg/s)
mh	Mass flow rates of the hot stream (kg/s)
Nc	Number of channels
Nch	Numbers of channels for the hot stream
Ncc	Numbers of channels for the cold stream
$Ncpc_{fc}$	Numbers of channels in a pass fc
$Ncph_{fh}$	Numbers of channels in a pass fh
Npc	Number of passes of the cold stream
Nph	Number of passes of the hot stream
Nt	Number of plates
Nu	Nusselt number
pc_{fc}	Orientation of the flow of the cold stream in the pass fc
ph_{fh}	Orientation of the flow of the hot stream in the pass fh
pn_n	Orientation of the stream that flows in a channel n
Pr	Prandtl numbers
$q_{n1,n2}$	Thermal flux between the channels $n1$ and $n2$ (W/m^2)
Re	Reynolds number
Rf	Fouling factor (m^2·K/W)
Sc	Set of the pairs of each channel and the corresponding cold pass
Sh	Set of the pairs of each channel and the corresponding hot pass
t	Plate thickness (m)
T_n	Stream temperature (°C)
Tci	Cold stream inlet temperature (°C)
$Thout_{fh}$	Outlet temperatures of the cold stream of the pass fc (°C)
Thi	Hot stream inlet temperature (°C)
$Thout_{fh}$	Outlet temperatures of the hot stream of the pass fh (°C)
$Tref$	Reference temperature (°C)
$Ts_{n1,n2}$	Surface temperature between channel $n1$ and $n2$ (°C)
$U_{n1,n2}$	Overall heat transfer coefficients between the channels $n1$ and $n2$ (W/(m^2·K))
y	Spatial coordinate along with the plate height (m)
β	Chevron angle (°)
μ	Stream viscosity at the bulk temperature (Pa·s)
μw	Stream viscosity at the wall temperature (Pa·s)
λ	Damping factor
ρ_n	Stream density (kg/m^3)
ϕ	Surface enlargement factor
Δy	Distance between adjacent grid elements (m)
ΔP_n	Pressure drop in a channel n (bar)
ΔPp	Pressure drop at the ports (bar)

Indexes

fh	Hot stream pass index
fc	Cold stream pass index
j	Mesh grid index
n	Channel index

addressed the simulation of gasketed-plate heat exchangers using numerical solutions of the conservation equations. Gut and Pinto [10] developed a mathematical model for plate heat exchanger simulation for any configuration, considering the variation of the physical properties for the energy balance and a simplified model using uniform values of the physical properties for the mechanical energy balance. Dardour et al. [6] presented the simulation of cocurrent heat exchangers based on the solution of the set of differential energy balances along the channels using a shooting method. Qiao et al. [28] presented a model that involves the discretization of the heat exchanger channels. The temperature profile in each segment is obtained assuming a fixed value of the wall temperature on both sides. The set of values of the wall temperatures is updated in an outer level of the convergence algorithm. Yoon and Jeong [35] developed a simulation scheme based on a network that considers a 2D flow field for the simulation of countercurrent heat exchangers, but other configurations were not addressed. Tabares et al. [33] employed the differential model of Gut and Pinto [10] for performance analysis of different configurations of heat exchangers. Jamil et al. [17] proposed a model based on the evaluation of the overall heat transfer coefficient using a numerical integration procedure. Examples of application of those more rigorous models, for design optimization based on the solution of the set of differential equations, can be found in Gut and Pinto [11], Mota [25], and Shokouhmand and Hasanpour [32].

The literature also contains several papers that addressed the simulation problem of gasketed-plate heat exchangers using computational fluid dynamics (CFD) [23,13,1,7,22,24]. However, despite the potentially higher accuracy associated with results obtained using CFD tools, they demand higher computational times, which hinders the utilization of CFD for design applications.

In this article, a generalized mathematical model is presented for the steady-state simulation of gasketed-plate heat exchangers. The model corresponds to a set of algebraic equations obtained from the discretization of the set of differential equations of the energy and mechanical energy balances along the heat exchanger channels. The model is presented for streams without phase change that flows through channels formed by Chevron plates, but the flexibility of the structure can be also extended for other alternatives.

The main contribution of the current paper is the generalized nature of the proposed model, composed of a single mathematical structure, which can represent any configuration of gasketed-plate heat exchanger, with any number of passes of the hot and cold streams. The selection of a given alternative is based on the set of a given group of model parameters. Another important aspect of the model is the absence of assumptions related to the uniformity of physical properties, therefore it can provide more accurate predictions than analytical solutions. Simulation results illustrate the impact of the use of these assumptions on the design, showing how conventional approaches, based on analytical solutions, can produce erroneous evaluations in certain situations.

A full generalization of the gasketed-plate heat exchanger model considering energy and mechanical energy balances, including the variation of the streams' physical properties with temperature, was not fully addressed in the literature before. Indeed, several models are limited to a given configuration like the models of Dardour et al. [6], Yoon and Jeong [35], and Jamil et al. [17], which are limited to co-

current or countercurrent heat exchangers. Other models depend on a specific formulation for each configuration: for example, Qiao et al. [28] proposed a matrix to generalize their model, but a fully parameterized representation of all equations was not presented. As mentioned above, Gut and Pinto [10] presented a generalized representation of the heat exchanger structure, but the variation of the physical properties with temperature was considered in the energy balance, but not in the mechanical energy balance. Consequently, Gut and Pinto [10] argued that the variation of the streams physical properties is not relevant; however, our results indicate that the simulation results may be affected by this issue considerably and must be explicitly addressed in the model.

This article is organized as follows. We first present the set of differential equations of the energy and mechanical energy balances. We then present the discretization procedure applied to the set of differential equations and the corresponding solution algorithm. We finish with sections of model validation, results, and conclusions.

2. Heat exchanger model

The heat exchanger model involves a set of parameters that represent the geometry of the heat exchanger. Based on this representation, the set of differential equations of the mathematical model encompasses a thermal model and a hydraulic model.

2.1. Heat exchanger structure representation

The structure of a gasketed-plate heat exchanger is illustrated in Fig. 1. This kind of heat exchanger is composed of a packed set of corrugated plates. A channel is formed between each pair of plates, such that, the hot and cold streams flow through these channels, and heat is transferred across the plates. The plates have gaskets that prevent the leak of the streams from the heat exchangers. The gaskets are also responsible to define which stream (hot or cold) flows in each channel.

The proposed model is based on a mathematical description of the configuration of the heat exchanger using a set of indices and parameters, as follows.

The total number of plates in a heat exchanger is represented by Nt, which defines $Nc = Nt - 1$ channels between plates, where the hot and cold streams flow. The numbers of channels for the cold and hot streams are equal to Nch and Ncc, respectively. Each channel is identified by the

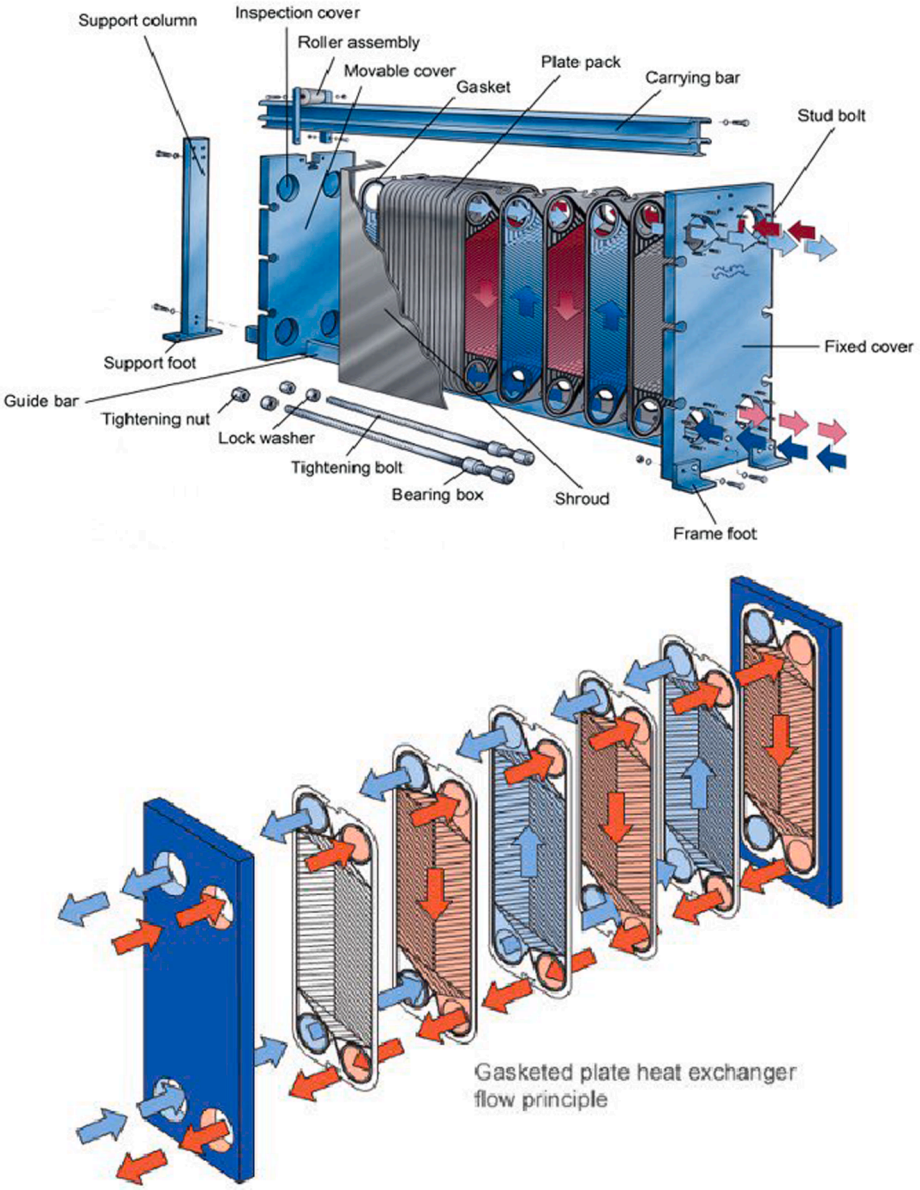

Fig. 1. Gasketed plate exchanger (Courtesy of Alfa Laval).

index $n = 1,\ldots, Nt-1$ (the first channel is next to the end of the hot stream inlet). The channels are organized in a way that adjacent channels always involve different streams, thus promoting the heat transfer across the heat exchanger plates. It is assumed that the hot and cold streams are fed at the opposite ends of the heat exchanger.

The number of channels associated with the hot and cold streams depends on the total number of plates and the identification of each stream flow in the first channel. If the hot stream flows in the first channel, then:

$$Nch = \text{ceil}((Nt-1)/2) \tag{1}$$

$$Ncc = \text{floor}((Nt-1)/2) \tag{2}$$

Otherwise:

$$Nch = \text{floor}((Nt-1)/2) \tag{3}$$

$$Ncc = \text{ceil}((Nt-1)/2) \tag{4}$$

The set of channels are distributed along different passes. The numbers of passes of the hot and cold streams are Nph and Npc. The different passes of the hot and cold streams are identified by the indices fh, such that, $fh = 1,\cdots, Nph$ for the hot streams and $fc = 1,\cdots, Npc$ for the cold streams. The passes are numbered from the end of the hot stream inlet. The numbers of channels in a pass fh and fc are represented by $Ncph_{fh}$ and $Ncpc_{fc}$, for hot and cold streams, respectively. These values are given by the following expression:

$$Ncph_{fh} = \begin{cases} \text{floor}(Nch/Nph), \text{for}(Nch \bmod Nph) = 0 \vee fh > (Nch \bmod Nph) \\ \text{floor}(Nch/Nph)+1, \text{otherwise} \end{cases} \tag{5}$$

$$Ncpc_{fc} = \begin{cases} \text{floor}(Ncc/Npc), \text{for}(Ncc \bmod Npc) = 0 \vee fc \le Npc - (Ncc \bmod Npc) \\ \text{floor}(Ncc/Npc)+1, \text{otherwise} \end{cases} \tag{6}$$

The orientation of the stream that flows in a channel n is given by the parameters pn_n. If $pn_n = +1$, then the flow in the channel n is upwards; otherwise $pn_n = -1$. Similarly, the orientation of the flow of the hot and cold streams in the pass fh and fc is given by the parameters ph_{fh} and pc_{fc}, respectively. The values of pn_n, ph_{fh} and pc_{fc} are automatically established according to the heat exchanger configuration, as shown below.

For any combination of the number of passes for the hot and cold stream, the identification of ph_{fh} and pc_{fc} is established according to the following relations (the orientation of the first pass for both streams is fixed according to the nozzle orientation):

$$ph_{fh} = -ph_{fh-1}, \text{ for } fh > 1 \tag{7}$$

$$pc_{fc} = -pc_{fc-1}, \text{ for } fc > 1 \tag{8}$$

Let Sh and Sc be the sets of the pairs of each channel and the corresponding hot and cold pass. These sets can be provided automatically by the following mathematical representation:

If the hot stream flows through the first channel:

$$Sh = \left\{ (n,fh) \left| 2\left(\sum_{fh'=1}^{p'-1} Ncph_{fh'}\right) < n \le 2\left(\sum_{fh'=1}^{p'} Ncph_{fh'}\right), \right.\right.$$

$$\left.\left. \text{for } (p' < fh) \text{ and } (n \bmod 2 = 1) \right\} \right. \tag{9}$$

$$Sc = \left\{ (n,fc) \left| 2\left(\sum_{fc'=1}^{p'-1} Ncpc_{fc'}\right) < n \le 2\left(\sum_{fc'=1}^{p'} Ncpc_{fc'}\right), \right.\right.$$

$$\left.\left. \text{for } (p' < fc) \text{ and } (n \bmod 2 = 0) \right\} \right. \tag{10}$$

If the cold stream flows through the first channel:

$$Sh = \left\{ (n,fh) \left| 2\left(\sum_{fh'=1}^{p'-1} Ncph_{fh'}\right) < n \le 2\left(\sum_{fh'=1}^{p'} Ncph_{fh'}\right), \right.\right.$$

$$\left.\left. \text{for } (p' < fh) \text{ and } (n \bmod 2 = 0) \right\} \right. \tag{11}$$

$$Sc = \left\{ (n,fc) \left| 2\left(\sum_{fc'=1}^{p'-1} Ncpc_{fc'}\right) < n \le 2\left(\sum_{fc'=1}^{p'} Ncpc_{fc'}\right), \right.\right.$$

$$\left.\left. \text{for } (p' < fc) \text{ and } (n \bmod 2 = 1) \right\} \right. \tag{12}$$

Now, the parameters pn_n are provided by:

$$pn_n = ph_{fh}, \text{ for } (n,fh) \in Sh \tag{13}$$

$$pn_n = pc_{fc}, \text{ for } (n,fc) \in Sc \tag{14}$$

Based on the proposed set of mathematical relations presented above, the system of equations for the simulation of a given heat exchanger is represented automatically, as shown below, no matter the number of passes for the hot and cold streams. For example, the heat capacity of the stream that flows in a channel n can be automatically accessed as follows:

$$Cp_n = Cph(T_n), \text{ for } (n,fh) \in Sh \tag{15}$$

$$Cp_n = Cpc(T_n), \text{ for } (n,fc) \in Sc \tag{16}$$

where Cph and Cpc are the heat capacities of the hot and cold streams, respectively. Similar relations can be established for any other physical property.

2.2. Thermal model

The dimensions of the plate are shown in Fig. 2, where Lw is the plate width inside gasket, Lp is the projected plate length, Lv is the vertical port distance, Dp is the port diameter, and β is the Chevron angle [18]. Based on this representation and the organization of adjacent channels in Fig. 3, the application of a differential energy balance [30] for a

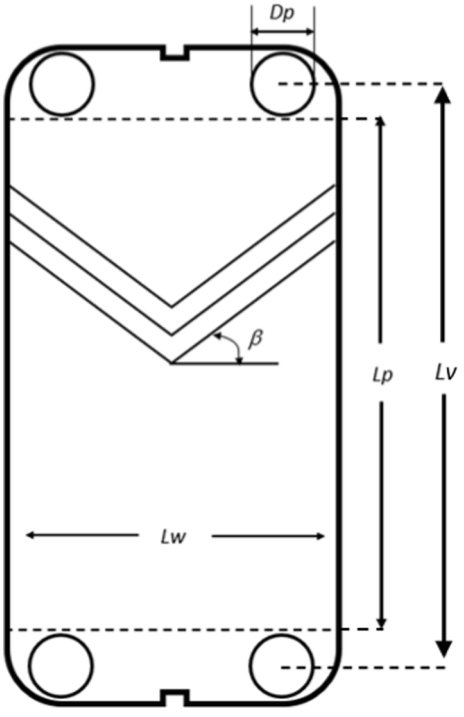

Fig. 2. Plate dimensions.

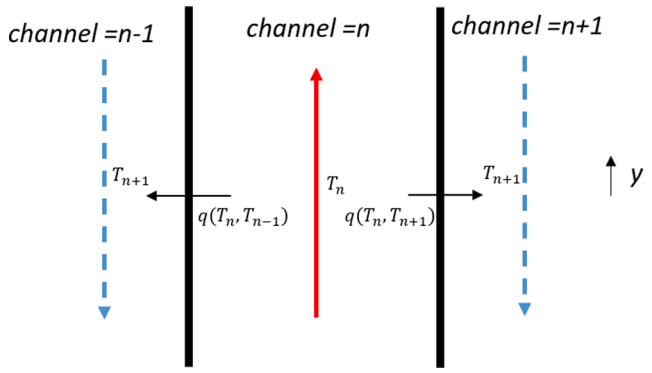

Fig. 3. Representation of adjacent channels.

generic channel n of a gasketed-plate heat exchanger yields (axial diffusion and viscous dissipation are dismissed):

$$\frac{dT_n}{dy} = -pn_n \frac{Lw\phi}{mc_n Cp_n}\left(q_{n,n-1} + q_{n,n+1}\right) \tag{17}$$

where T_n is the stream temperature, Cp_n is the heat capacity, y is the spatial coordinate along with the plate height (upwards), ϕ is the surface enlargement factor, mc_n is the mass flow rate in the channel, $q_{n,n-1}$ is the thermal flux between the channels n and $n-1$ and $q_{n,n+1}$ is the thermal flux between the channels n and $n+1$.

The mass flow rate in the channel n is calculated by the following expressions for the hot and cold streams:

$$mc_n = \frac{mh}{Ncph_{fh}}, \text{ for } (n, fh) \in Sh \tag{18}$$

$$mc_n = \frac{mc}{Ncpc_{fc}}, \text{ for } (n, fc) \in Sc \tag{19}$$

where mh and mc are the mass flow rates of the hot and cold streams.

The thermal flux between the channels in Eq. (17) are given by:

$$q_{n,n-1} = U_{n,n-1}(T_n - T_{n-1}) \tag{20}$$

$$q_{n,n+1} = U_{n,n+1}(T_n - T_{n+1}) \tag{21}$$

where $U_{n,n-1}$ and $U_{n,n+1}$ are the overall heat transfer coefficients between the channels n and $n-1$, and n and $n+1$, respectively. In addition, since the first and last plates are adiabatic walls, the thermal flux is equal to zero for both, that is:

$$q_{1,0} = 0 \tag{22}$$

$$q_{N_c, N_c+1} = 0 \tag{23}$$

The expression for evaluation of the overall heat transfer coefficient between adjacent channels n and $n-1$ is (an equivalent expression for $U_{n,n+1}$ is straightforward):

$$U_{n,n-1} = \frac{1}{\frac{1}{h_{n-1}} + Rf_{n-1} + \frac{t}{kw} + Rf_n + \frac{1}{h_n}} \tag{24}$$

where h is the convective heat transfer coefficient, Rf is the fouling factor, t is the plate thickness, and kw is the thermal conductivity of the plate material.

The evaluation of the convective heat transfer coefficient depends on the mass flux in the channel and the temperature. Any proper correlation for the evaluation of heat transfer coefficients in gasketed-plate heat exchangers can be employed here. Jamil et al. [16] present several options available in the literature. In general, these correlations are represented by:

$$Nu = Nu(Re, Pr) \tag{25}$$

where Nu, Re, and Pr are the Nusselt, Reynolds, and Prandtl numbers.

Additionally, some correlations also involve a correction factor expressed by a ratio of the stream viscosity at the bulk temperature and at the wall: $(\mu/\mu w)^{0.14}$ or $(\mu/\mu w)^{0.17}$. Using the concept of hydraulic diameter, the expressions of the dimensionless groups present in Eq. (25) are:

$$Nu = \frac{hD_{hyd}}{k} \tag{26}$$

$$Re = \frac{D_{hyd}G}{\mu} \tag{27}$$

$$Pr = \frac{Cp\mu}{k} \tag{28}$$

where D_{hyd} is the hydraulic diameter, k is the stream thermal conductivity and G is the mass flux in the channel. The expression for the evaluation of the mass flux in a channel n is given by:

$$G_n = \frac{mc_n}{b\ Lw} \tag{29}$$

where b is the mean channel spacing.

If the heat transfer coefficient correlation contains the correction term based on the ratio between the viscosities at the bulk temperature and at the surface temperature, the model is complemented by the equation for the evaluation of the surface temperature. Thus, the surface temperature between channel n and $n-1$, represented by $Ts_{n,n-1}$ (an equivalent expression for $Ts_{n,n+1}$ is straightforward) is the following:

$$\frac{T_{n-1} - T_n}{\frac{1}{h_{n-1}} + Rf_{n-1} + \frac{t}{kw} + Rf_n + \frac{1}{h_n}} = \frac{Ts_{n,n-1} - T_n}{\frac{1}{h_n}} \tag{30}$$

2.3. Hydraulic model

The hydraulic model addresses the pressure drop associated with friction losses of the flow along the channels. The pressure drop in a channel n can be evaluated using the Darcy–Weisbach, represented below in a differential form [30]:

$$\frac{dP_n}{dy} = \frac{f_n G_n^2}{2D_{hyd}\rho_n} \tag{31}$$

where f is the friction factor, which depends on the Reynolds number. Several correlations presented in the literature for evaluation of the friction factor are reported in Jamil et al. [16].

3. Discretized model

The differential equations of the thermal and hydraulic models were discretized using the midpoint method. The resultant equations are shown below together with some additional algebraic equations that complement the heat exchanger mathematical model.

3.1. Thermal model

According to the grid representation displayed in Fig. 4, the algebraic equation resultant from the discretization of Eq. (17) is given by:

$$\frac{T_{n,j} - T_{n,j-1}}{\Delta y} = -p_n \frac{Lw\ \widehat{\varnothing}}{mc_n\ Cp_{n,j,j-1}}\left(q_{n-1,n,j,j-1} + q_{n,n+1,j,j-1}\right), \text{ for } j = 2, \cdots, J \tag{32}$$

where j in the grid index and Δy is the distance between adjacent grid elements ($\Delta y = Lp/(J-1)$). According to the midpoint method employed in the derivative discretization [5], $Cp_{n,j,j-1}$, $q_{n-1,n,j,j-1}$, $q_{n,n+1,j,j-1}$ are evaluated considering the average of the temperatures at the points j and $j-1$: $(T_{n,j} + T_{n,j-1})/2$.

Initial conditions of the temperature at the inlet of each channel have to be provided. For the first pass along the flow ($fh = 1$ and $fc = Npc$), the

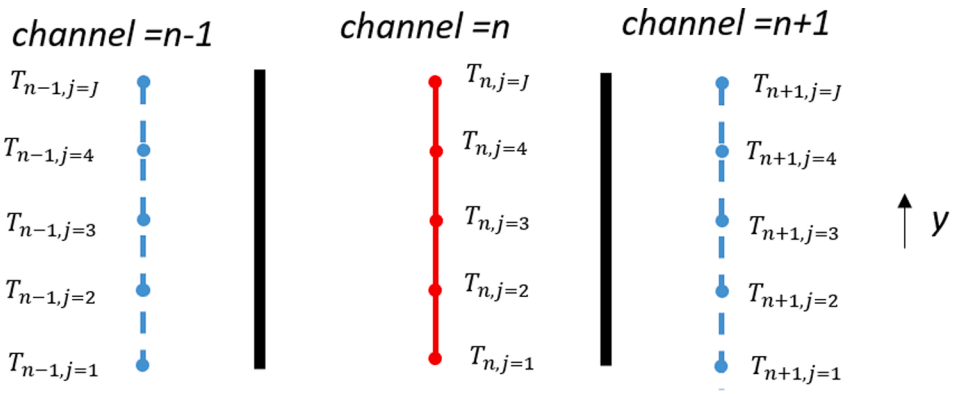

Fig. 4. Numerical grid of the thermal model.

initial conditions are given by:

$$T_{n,1} = Thi,\ \text{for}\ (n,1) \in Sh\ \text{and}\ ph_1 = 1 \tag{33}$$

$$T_{n,J} = Thi,\ \text{for}\ (n,1) \in Sh\ \text{and}\ ph_1 = -1 \tag{34}$$

$$T_{n,1} = Tci,\ \text{for}\ (n,Npc) \in Sc\ \text{and}\ pc_{Npc} = 1 \tag{35}$$

$$T_{n,J} = Tci,\ \text{for}\ (n,Npc) \in Sc\ \text{and}\ pc_{Npc} = -1 \tag{36}$$

where *Thi* and *Tci* are the hot and cold stream inlet temperatures, respectively.

The inlet temperature for channels belonging to the further passes is equal to the outlet temperature of the previous pass along the flow:

$$T_{n,1} = Thout_{fh-1},\ \text{for}\ (n,fh) \in Sh,\ fh > 1\ \text{and}\ ph_{fh} = 1 \tag{37}$$

$$T_{n,J} = Thout_{fh-1},\ \text{for}\ (n,fh) \in Sh,\ fh > 1\ \text{and}\ ph_{fh} = -1 \tag{38}$$

$$T_{n,1} = Tcout_{fc+1},\ \text{for}\ (n,fc) \in Sc,\ fc < Npc\ \text{and}\ pc_{fc} = 1 \tag{39}$$

$$T_{n,J} = Tcout_{fc+1},\ \text{for}\ (n,fc) \in Sc,\ fc < Npc\ \text{and}\ pc_{fc} = -1 \tag{40}$$

where $Thout_{fh}$ and $Tcout_{fc}$ are the outlet temperatures of the hot and cold streams of the pass *fh* and *fc*, respectively.

The expressions for evaluation of $Thout_{fh}$ and $Tcout_{fc}$ are:

$$\left(\sum_{(n,fh)\in Sh} mc_n \int_{Tref}^{Thout_{fh}} Cp_n(T)dT\right) = \left(\sum_{(n,fh)\in Sh} mc_n \int_{Tref}^{T_{n,J}} Cp_n(T)dT\right),\ \text{for}\ ph_{fh} = +1 \tag{41}$$

$$\left(\sum_{(n,fh)\in Sh} mc_n \int_{Tref}^{Thout_{fh}} Cp_n(T)dT\right) = \left(\sum_{(n,fh)\in Sh} mc_n \int_{Tref}^{T_{n,1}} Cp_n(T)dT\right),\ \text{for}\ ph_{fh} = -1 \tag{42}$$

$$\left(\sum_{(n,fc)\in Sc} mc_n \int_{Tref}^{Tcout_{fc}} Cp_n(T)dT\right) = \left(\sum_{(n,fc)\in Sc} mc_n \int_{Tref}^{T_{n,J}} Cp_n(T)dT\right),\ \text{for}\ pc_{fc} = +1 \tag{43}$$

$$\left(\sum_{(n,fc)\in Sc} mc_n \int_{Tref}^{Tcout_{fc}} Cp_n(T)dT\right) = \left(\sum_{(n,fc)\in Sc} mc_n \int_{Tref}^{T_{n,1}} Cp_n(T)dT\right),\ \text{for}\ pc_{fc} = -1 \tag{44}$$

where *Tref* is a reference temperature to calculate the stream enthalpy. These expressions are also responsible for the evaluation of the outlet temperatures of the hot and cold streams, i.e. $Thout_{Nph}$ and $Tcout_1$.

3.2. Hydraulic model

The nodes of the grid for the discretization of the friction loss equation are located in the same position as the thermal grid, as illustrated in Fig. 5. The discretization of the friction losses along with the plate in Eq. (31) using the midpoint method, according to this grid yields:

$$\frac{P_{n,j} - P_{n,j-1}}{\Delta y} = \frac{f_{n,j,j-1} G_n^2}{2 D_{hyd} \rho_{n,j,j-1}},\ \text{for}\ j = 2, \cdots, J \tag{45}$$

where the friction factor, $f_{n,j,j-1}$ and the density $\rho_{n,j,j-1}$ in Eq. (45) are evaluated using the corresponding physical properties calculated at the average temperature $(T_{n,j} + T_{n,j-1})/2$.

Eq. (45) expresses the pressure drop between the grid nodes $j = 1$ and $j = J$, however, the effective flow length (*Lv*) is different from the effective heat transfer length (*Lp*) [18], therefore, additional segments above and below the original grid must be added, indicated here as $j = 0$ and $j = J + 1$. The pressure drop in these segments is given by:

$$\frac{P_{n,J+1} - P_{n,J}}{(Dp/2)} = \frac{f_{n,J+1,J} G_n^2}{2 D_{hyd} \rho_{n,J+1,J}} \tag{46}$$

$$\frac{P_{n,1} - P_{n,0}}{(Dp/2)} = \frac{f_{n,1,0} G_n^2}{2 D_{hyd} \rho_{n,1,0}} \tag{47}$$

Dismissing the heat transfer above node *j* and below node 1, the evaluation of the friction factor and the density in Eq. (46) and Eq. (47) is based on $T_{n,J+1} = T_{n,J}$ and $T_{n,1} = T_{n,0}$.

Based on Eqs. (45–47), the pressure drop in a channel *n* is given by:

$$\Delta P_n = P_{J+1} - P_0 \tag{48}$$

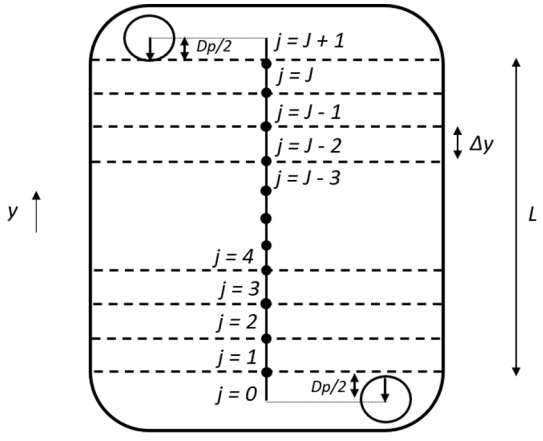

Fig. 5. Numerical grid of the hydraulic model.

The variation of the physical properties with temperature implies different calculated values of the pressure drop in the channels of the same pass according to Eq. (48), thus the pressure drop of the flow in a heat exchanger pass is calculated by an average value of their channels (the proposed model does not address effects related with the nonuniformity of the flow rates along different channels of the same pass):

$$\Delta Ph_{fh} = \sum_{n} \frac{\Delta P_n}{Ncph_{fh}}, \text{for } (n, fh) \in Sh \tag{49}$$

$$\Delta Pc_{fc} = \sum_{n} \frac{\Delta P_n}{Ncpc_{fc}}, \text{for } (n, fc) \in Sc \tag{50}$$

Finally, the hot and cold streams' pressure drops correspond to the sum of the pressure drop in each pass summed with the pressure drop at the ducts that formed the ports [18]:

$$\Delta Ph = \sum_{fh} \Delta Ph_{fh} + \Delta Pph \tag{51}$$

$$\Delta Pc = \sum_{fc} \Delta Pc_{fc} + \Delta Ppc \tag{52}$$

where ΔPp is the pressure drop at the ports.
The pressure drop in the port is given by:

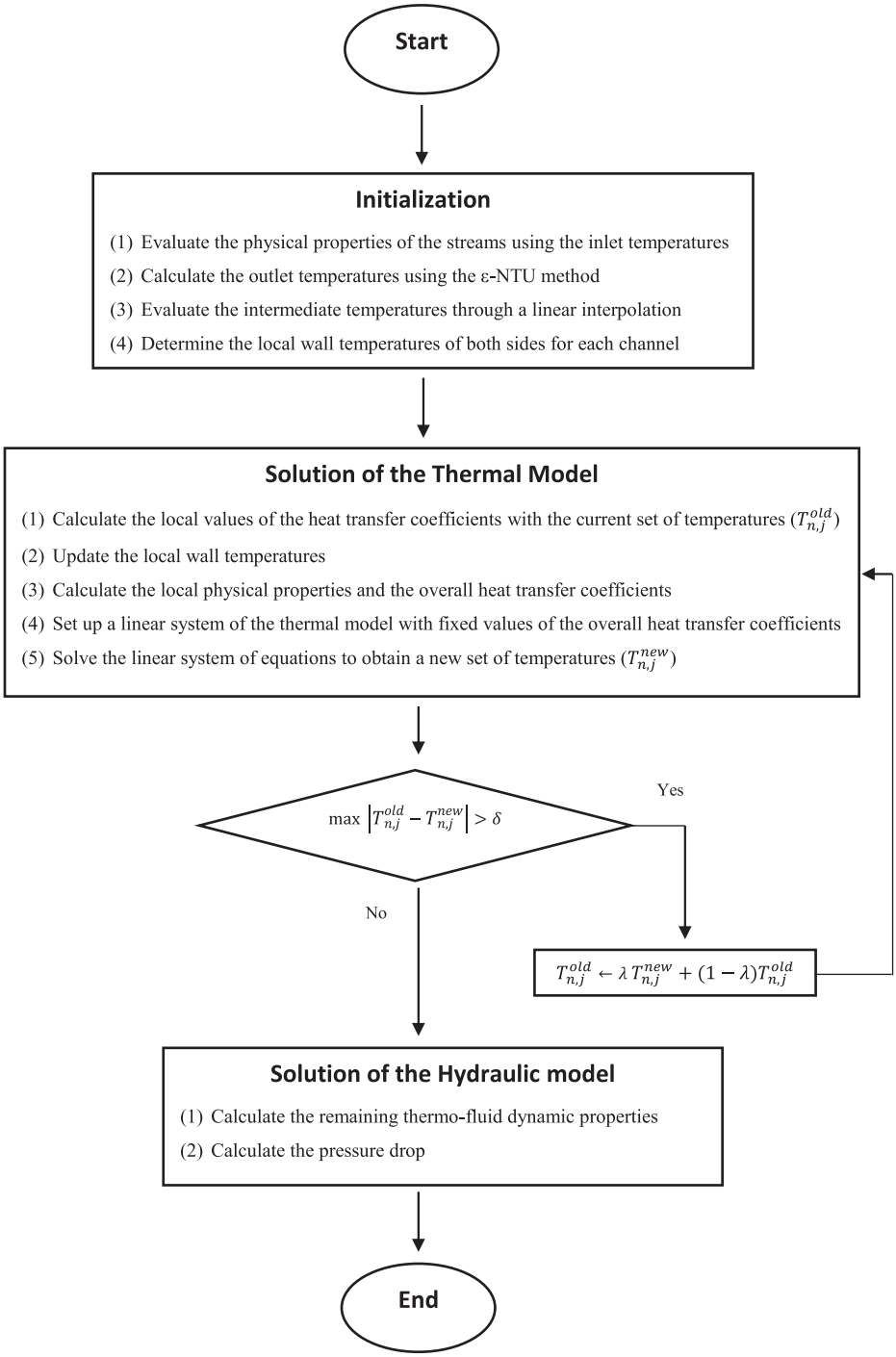

Fig. 6. Simulation algorithm.

$$\Delta P_p = 1.4Np\frac{Gp^2}{2\rho} \tag{53}$$

where ρ is the stream density calculated with the average temperature between the inlet and outlet conditions, and Gp is the mass flux through the port.

$$Gp = \frac{m}{\left(\frac{\pi Dp^2}{4}\right)} \tag{54}$$

4. Solution procedure

The proposed simulation scheme of gasketed-plate heat exchangers involves the solution of the thermal model (Eqs. 32–44), followed by the solution of the hydraulic model (Eqs. 45–54). Because of the variation of the physical properties with temperature, the thermal model is nonlinear and it is solved through an iterative procedure. The initial estimate for the convergence of this iterative procedure is generated automatically using a countercurrent ε-NTU model. The hydraulic model is linear and it is solved directly, without the need for initial estimates. The structure of the simulation scheme is shown in Fig. 6. Convergence is usually achieved in a few iterations. However, in a few cases, oscillation between two set of values was observed. Thus, a damping factor in the temperature update was added: $\lambda = 1$ until the fifth iteration and $\lambda = 0.5$ for the subsequent iterations.

5. Validation

The validation of the proposed simulation scheme was tested comparing its results with three different sources:

(1) Closed-form equations valid for an infinite number of plates.
(2) Numerical simulation results available in the literature.
(3) Experimental data.

The correlation for evaluation of the convective heat transfer coefficients employed in these validations are present in Saunders [31] (see Supplementary Material). The validations (1) and (2) considered uniform physical properties, following the nature of the original data. Validation (3) employed the variation of the physical properties with temperature.

5.1. Comparison with closed forms valid for an infinite number of plates

Kandlikar and Shah [19] presented ε-NTU closed-form relations for several gasketed-plate heat exchanger configurations with an infinite number of plates, i.e. without the effects related to end plates and the channels between adjacent passes. According to Kandlikar and Shah [20], these effects are less significant for a number of thermal plates higher than 40. Therefore, the results of the proposed simulation for heat exchangers with a large number of plates are compared with equivalent evaluations using the ε-NTU closed-form relations. The heat exchanger data are present in Table 1, corresponding to a Chevron plate with dimensions equivalent to a GEA VT-1306 plate [3]. The streams data are present in Table 2.

Table 3 shows the comparison of the simulation results considering four different heat exchanger configurations 1–1, 2–1, 1–2, 2–2. The average absolute relative difference between the evaluated heat loads using both approaches is equal to 0.17 %.

Table 1
Heat exchanger data.

Parameter	Value
Number of plates	201
Projected plate length, *Lp* (m)	0.978
Plate width inside gasket, *Lw* (m)	0.812
Corrugation type	Chevron
Chevron angle, β (°)	30
Port diameter, *Dp* (m)	0.288
Plate thickness, *t* (m)	0.0008
Flow channel gap, *b* (m)	0.003
Enlargement factor, ϕ	1.15
Plate thermal conductivity, *kw* (W/(m·K))	16.2

5.2. Comparison with numerical simulation results available in the literature

Kandlikar and Shah [20] presented simulation results based on a numerical solution of the energy balance equations using a finite difference procedure. These results are displayed through graphs of the LMTD correction factor and thermal effectiveness considering different numbers of plates for different configurations. These results are asymptotically equal to those presented in Kandlikar and Shah [19] for a large number of plates.

Our proposed approach attains equivalent results as in the graphs displayed by Kandlikar and Shah [19]. For example, Fig. 7 displays a graph of the LMTD correction factor curves generated through the proposed simulation scheme for a different number of plates in a heat exchanger with 2 passes for the hot stream and 1 pass for the cold stream ($pc_1 = 1$, $ph_1 = 1$). This graph also contains a set of discrete data points from Kandlikar and Shah [19], that match with the curve (the mean relative absolute error is 0.075 %). Thus, we conclude that the results obtained using both approaches are equivalent.

5.3. Comparison with experimental data

Yildiz and Ersöz [34] presented a dataset of 30 experimental runs from the countercurrent gasketed plate heat exchanger described in Table 4, associated with hot and cold water streams.

The results of the simulation of the 30 runs using the proposed scheme are compared with experimental data in Fig. 8. The physical properties of the water streams employed in the simulation are represented by mathematical functions fitted to experimental data (see Supplementary Material).

The graph in Fig. 8 shows a good match between the model predictions and the experimental data. The average absolute errors of the outlet temperatures are 1.70 °C and 0.87 °C, for the hot and cold streams, respectively. A numerical simulation provided by the same authors of the experimental data attained almost identical average errors (1.69 °C and 0.86 °C).

6. Results

We first show details of simulation results using the proposed procedure and limitations of the analytical solutions usually employed in optimization studies, and next, we discuss the importance of the accuracy of the model when used in a design problem. The evaluation of the convective heat transfer coefficients in these results was based on the correlations presented by Saunders [31] (see Supplementary Material).

Table 2
Streams data.

	Hot stream	Cold stream
Stream	Water	Water
Mass flow (kg/s)	40	40
Inlet temperature (°C)	146.9	91.9
Density (kg/m^3)	919.1	963.4
Heat capacity (J/(kg·K))	4302	4209
Dynamic viscosity (Pa·s)	$0.185{\cdot}10^{-3}$	$0.306{\cdot}10^{-3}$
Thermal conductivity (W/(m·K))	0.688	0.677
Fouling factor (m^{2}K/W)	0.0004	0.0002

Table 3
Heat load results.

Configuration (Number of passes: Hot stream – Cold stream)	Heat load evaluated using ε-NTU closed-form relations (kW)	Heat load evaluated using the proposed model (kW)	Absolute relative difference (%)
(1–1) $pc_1 = -1$, $ph_1 = 1$	5296.6	5289.9	0.13
(2–1) $pc_1 = -1$, $ph_1 = 1$	4900.1	4889.3	0.22
(1–2) $pc_1 = 1$, $ph_1 = 1$	4911.8	4903.7	0.16
(2–2) $pc_1 = 1$, $ph_1 = 1$	5478.4	5468.7	0.18

6.1. Simulation results and analysis of the limitations of analytical solutions

The gasketed-plate heat exchanger described in Table 5 is employed to illustrate the proposed simulation approach. The plate dimensions are equivalent to an Alfa Laval A35 plate [4].

The hot and cold streams correspond to engine oil, which presents a considerable variation of the viscosity with temperature. The physical properties of the streams are calculated in the simulation using mathematical functions fitted to the set of data in different temperatures presented by Incropera and DeWitt [15] (See Supplementary Material).

To show the importance of the utilization of the proposed approach for the simulation of gasketed-plate heat exchangers, the results are compared with analytical solutions obtained using the ε-NTU method and the evaluation of the pressure drop using the Darcy–Weisbach equation with uniform values of the physical properties. As discussed above, this approach was employed in several papers about heat exchanger design optimization [12,14,29].

The uniform values of the physical properties employed in the simulations using analytical solutions are evaluated in two ways. Alternative I uses physical properties calculated employing the average temperature of the inlet and outlet temperatures (Property Value = Property((*Tin* + *Tout*)/2)). Alternative II uses average values of the physical properties calculated employing the inlet and outlet temperatures (Property Value = (Property(*Tin*) + Property(*Tout*))/2). Following the procedure proposed by Gut and Pinto [10], the outlet temperature employed for evaluation of the physical properties corresponds to an estimative associated with a heat exchanger effectiveness equal to 0.75.

The simulation code was written in Python employing the module NumPy for fast array manipulations and the module SciPy for handling sparse matrices. The results presented below are associated with a discretization grid of the differential equations containing 25 points. The resultant computational time needed for each simulation is small, varying from 0.03 *sec* for small units to 1.5 *sec* for large ones, using a personal computer with a processor i7-8565U 1.8 GHz and 8 GB of RAM memory.

The simulation using the proposed procedure yields the temperature profiles along the different channels of the two passes of the heat exchanger depicted in Fig. 9. The profiles are coherent with the flow orientation in each pass. Due to the small number of plates, each channel has a different temperature profile: the channels nearer to the heat exchanger ends are associated with smaller temperature variations. It is possible to observe in the set of profiles that the inlet temperature of the second pass for each stream corresponds to an intermediate value among the outlet temperatures of the different channels of the first pass, due to the energy balance resultant from the mixture of the streams at the outlet of each pass.

The outlet temperature and pressure drop evaluated using the proposed simulation procedure are presented in Table 6. The temperature deviations between the results of our proposed simulation approach and the analytical solutions are relatively small for this heat exchanger example, but the deviations associated with the pressure drop are large.

Table 4
Heat exchanger data.

Parameter	Value
Number of plates	15
Total effective area, m^2	0.1968
Plate width inside gasket, *Lw* (m)	0.080
Corrugation type	Chevron
Chevron angle, β (°)	45
Port diameter, *Dp* (m)	0.016
Plate thickness, *t* (m)	0.0003
Flow channel gap, *b* (m)	0.00325
Enlargement factor, ϕ	1.273
Plate thermal conductivity, *kw* (W/(m·K))	17.5

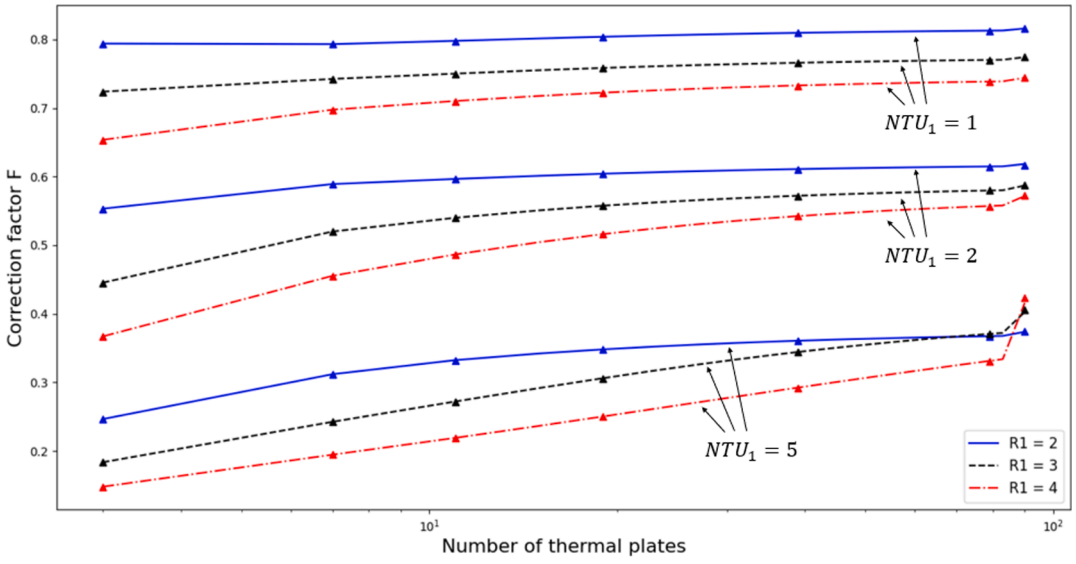

Fig. 7. Correction factor curves for different number of plates: $R_1 = (\dot{m}_c Cp_c)/(\dot{m}_h Cp_h)$ and $NTU_1 = UA/(\dot{m}_c Cp_c)$.

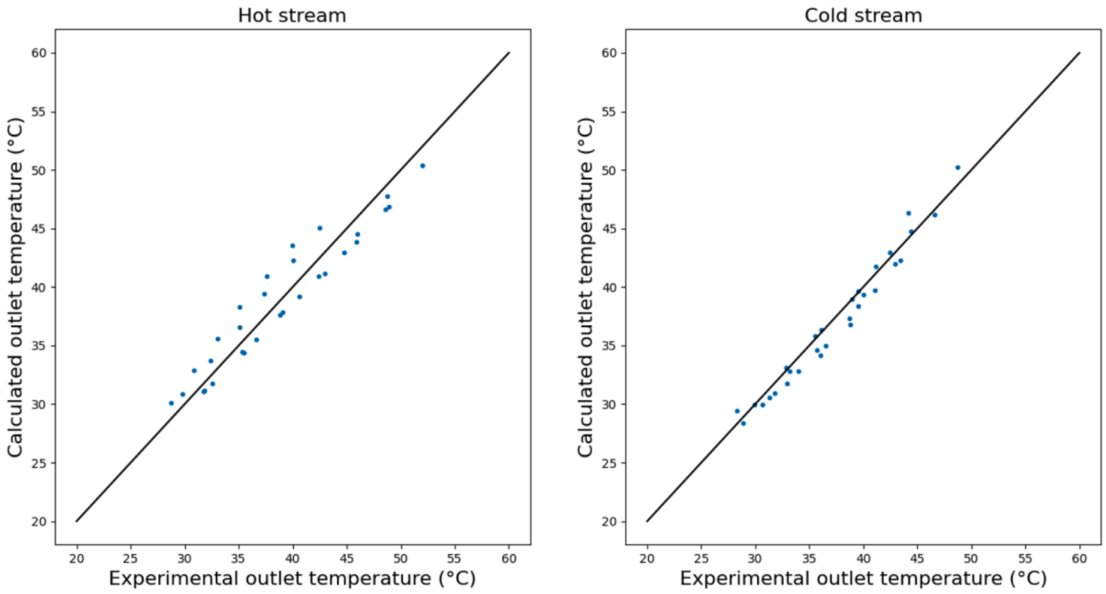

Fig. 8. Scatter plots of calculated versus measured outlet temperatures.

Table 5
Heat exchanger example data.

Parameter	Hot stream	Cold stream
Stream	Engine oil	Engine oil
Mass flow (kg/s)	2.0	1.8
Inlet temperature (°C)	160	42
Number of passes	2	2
Number of plates	11	
Projected plate length, *Lp* (m)	1.500	
Plate width inside gasket, *Lw* (m)	1.220	
Corrugation type	Chevron	
Chevron angle, β (°)	45	
Port diameter, *Dp* (m)	0.35	
Plate thickness, *t* (m)	0.0008	
Flow channel gap, *b* (m)	0.003	
Enlargement factor, ϕ	1.15	
Plate thermal conductivity, *kw* (W/(m·K))	16.1	

For example, the cold stream pressure drop evaluated using properties calculated at an average temperature (Alternative I) is 27 % lower than the result obtained using the proposed numerical solution and the pressure drop evaluated using physical properties calculated through an

Table 6
Simulation results using different approaches.

	Proposed approach	Analytical solution	
		Alternative I	Alternative II
Hot stream outlet temperature (°C)	99.4	96.3	102.4
Hot stream pressure drop (bar)	0.77	0.67	0.94
Cold stream outlet temperature (°C)	116.2	117.6	110.3
Cold stream pressure drop (bar)	1.44	1.05	2.89

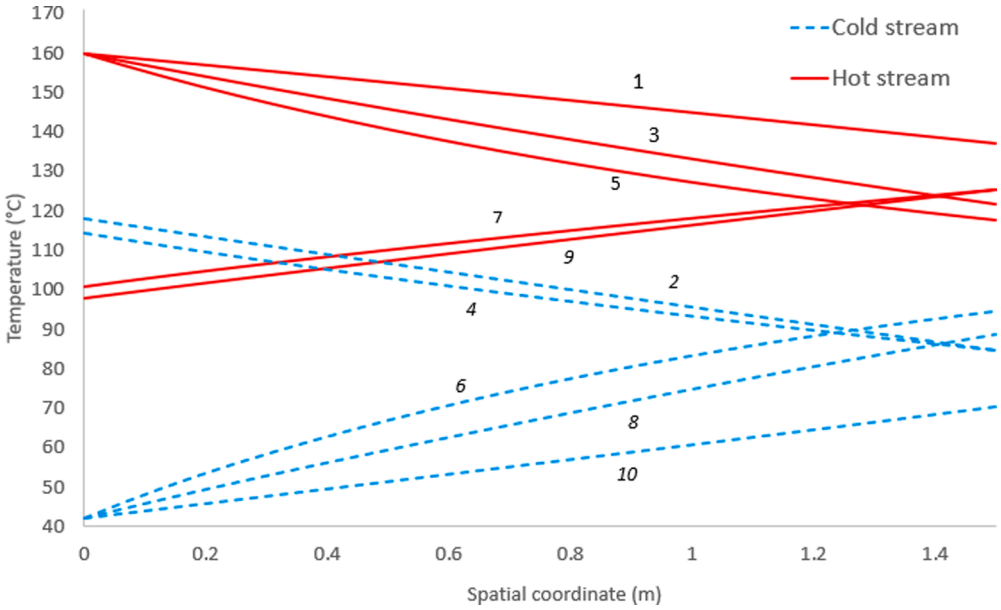

Fig. 9. Temperature profiles along the different channels of the heat exchanger.

average of the inlet and outlet values (Alternative II) is 101 % higher than the equivalent results using the proposed procedure.

The large differences in the cold stream pressure drop displayed in Table 6 can be illustrated by the corresponding pressure drop profiles. Fig. 10 presents the cold stream pressure drops along the spatial coordinate in channel 6 (one of the channels of the first pass). The pressure drop profiles evaluated using Alternatives 1 and 2 are linear, because of the assumption of uniform physical properties. However, the pressure drop profile obtained using the proposed approach is a curve associated with a decrescent gradient, due to the increase of the temperature that brings a viscosity reduction. The resultant pressure drop using the proposed approach is an intermediate value between the results of Alternatives 1 and 2.

This intermediate value of the pressure drop evaluated through the proposed approach can be explained by the cold stream viscosity profiles described in Fig. 11. This figure shows a comparison between the cold stream viscosity variation with temperature and the average values used in the simulation based on Alternatives I and II. It can be observed that these average values calculated using Alternatives I and II underestimate and overestimate the nonlinear variation of the viscosity with temperature in a large portion of the heat exchanger, which causes the corresponding deviations in the pressure drop evaluation.

An equivalent comparison of the data displayed in Table 6 was also made using 1920 different heat exchangers with an area ranging from 5.78 m^2 to 68.9 m^2. The deviations of the heat load and pressure drops are illustrated in Figs. 12, 13, and 14, where the ratio of the analytical solution values and our results is plotted as a function of the area. Fig. 12 indicates that the majority of the analytical solutions using Alternative I overestimates the heat load when compared with the proposed approach. An opposite trend is verified when Alternative II is employed, where the majority of the simulations underestimates the heat load. Figs. 13 and 14 show that the pressure drop deviations are more severe, with solutions overpredicting and underpredicting the pressure drop.

6.2. *Importance of the model accuracy for design*

Inaccurate simulations used during design procedures may imply the rejection of a lower-cost heat exchanger that would be adequate for the design task or, even worse, the adoption of a design solution that will not attain the desired performance during its operation, with considerable economic penalties. In the literature, there are two modeling approaches used for the design optimization of gasketed-plate heat exchangers: one is the use of analytical models based on uniform properties [37,9,26,12,14,29] and the other approach is the use of discretized models with constant physical properties, which can address end plate effects [11,25].

The importance of the utilization of the proposed model in design activities is illustrated using the data of the streams present in Table 5. The objective is to heat the cold stream of this example to 140 °C, limited to a maximum pressure drop of 0.6 bar in both streams. Our proposed simulation results are compared with a numerical solution obtained using uniform physical properties (Alternatives I and II are also tested here). These simplified models we refer to are equivalent to the ones employed by Gut and Pinto [11] and Mota et al. [25].

We accessed the simulation results of the sample of 1920 heat exchangers using different approaches and checked if each heat exchanger is suitable for the targeted duty. Based on these results, the accuracy limitations of the simplified models for this design task are quantified by the number of false-positive and false-negatives. A false positive is a heat exchanger that is feasible for the design task according to the simplified model, but it is not feasible when analyzed using the proposed full model. A false negative is a heat exchanger that is considered unfit for the design task by the simplified model, but it is feasible when tested using the proposed procedure.

Table 7 shows the distribution of the number of false positives and false negatives, depending on how the physical properties were evaluated. These results indicate that more than 10 % and 20 % of the heat exchangers present in the investigated sample would not be adequately analyzed as a candidate solution for the design problem using Alternatives I and II for the evaluation of the uniform values of the physical properties, respectively.

7. Conclusions

This paper presented a generalized mathematical model for the simulation of gasketed-plate heat exchangers. The model is composed of a single parameterized structure that can be employed to simulate heat exchangers with any number of passes for the hot and cold streams. Additionally, the variation of the physical properties with temperature is addressed explicitly in the model.

The validity of the model was successfully checked through the comparison of simulation outputs with three different results from the literature: closed-form equations valid for an infinite number of plates, numerical simulation data, and experimental data.

Numerical results showed that approaches based on uniform values of the physical properties are associated with considerable deviations

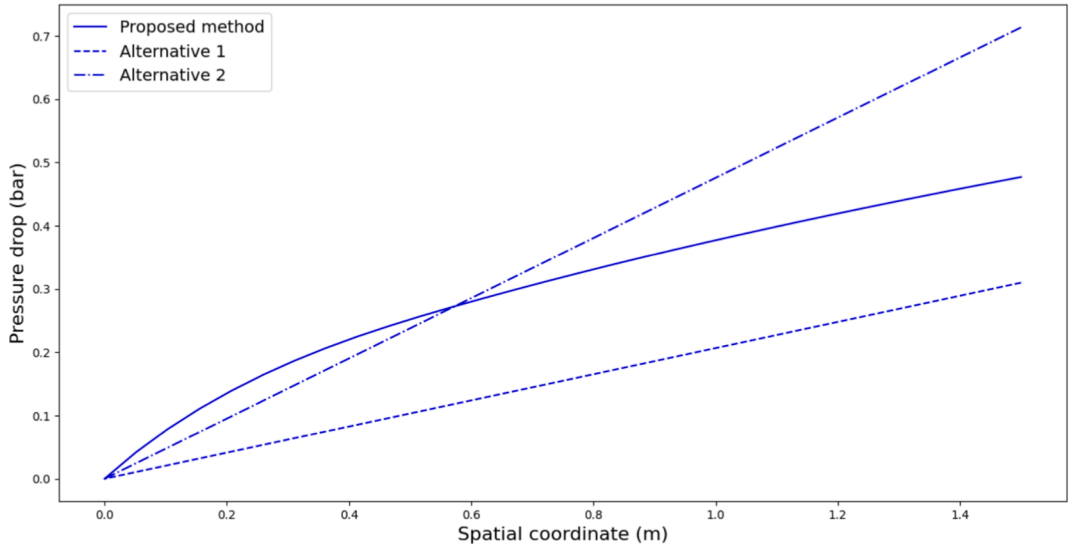

Fig. 10. Cold stream pressure drop profiles along channel 6.

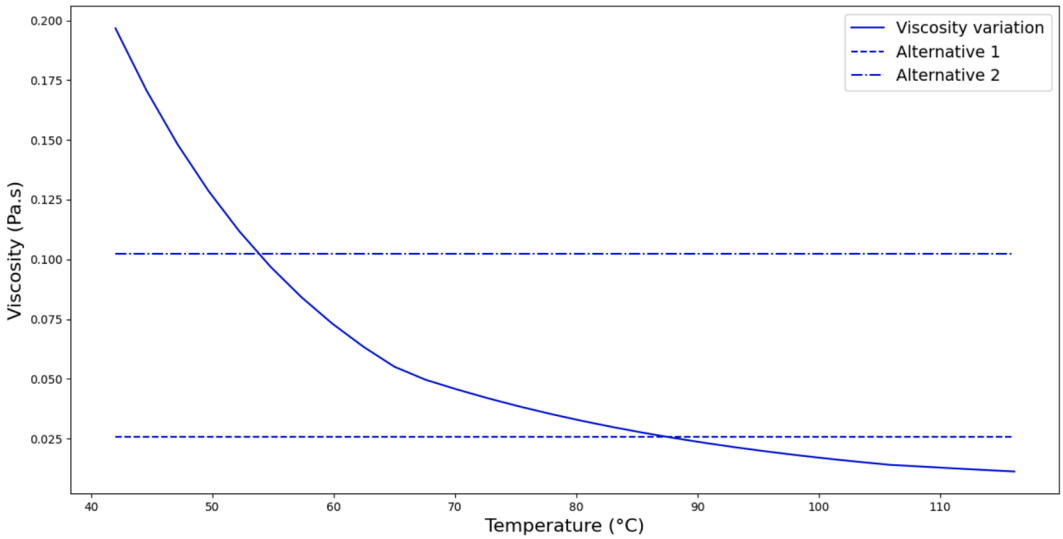

Fig. 11. Variation of the viscosity with temperature.

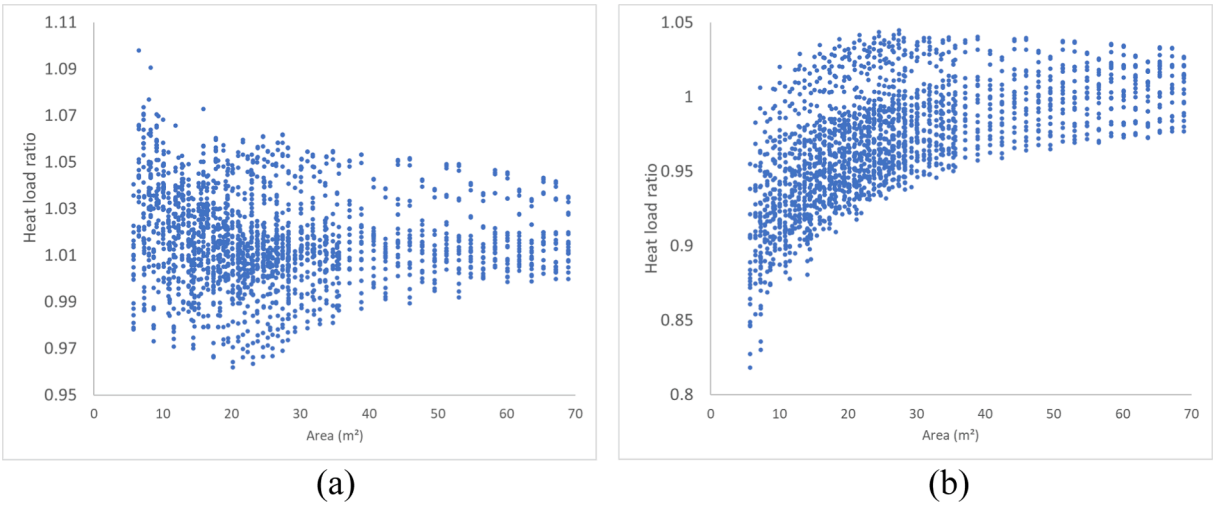

Fig. 12. Ratio between the heat load evaluated using an analytical solution and the proposed approach for the investigated set of heat exchangers. (a) Alternative I, (b) Alternative II.

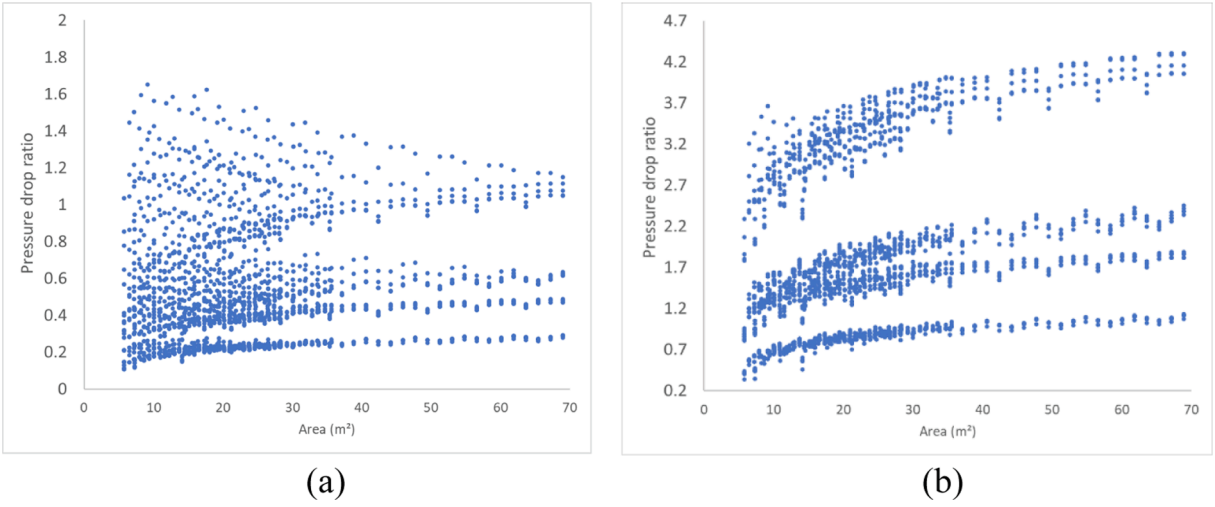

Fig. 13. Ratio between the cold stream pressure drop evaluated using an analytical solution and the proposed approach for the investigated set of heat exchangers. (a) Alternative I, (b) Alternative II.

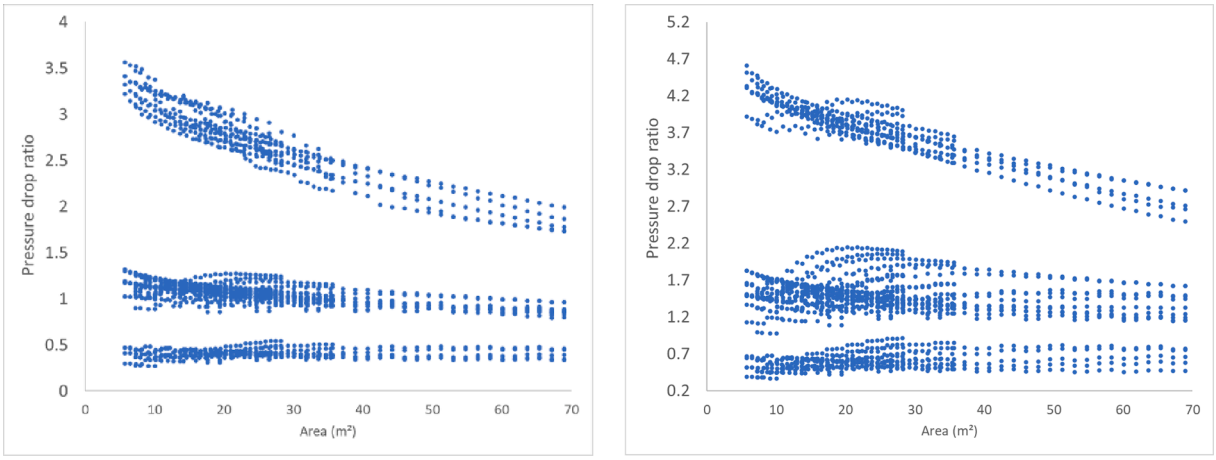

Fig. 14. Ratio between the hot stream pressure drop evaluated using an analytical solution and the proposed approach for a set of heat exchangers. (a) Alternative I, (b) Alternative II.

Table 7
Distribution of false positives and false negatives for the design.

	Simplified model	
	Alternative I	Alternative II
False positives	211 (11.0 %)	0 (0.0 %)
False negatives	4 (0.21 %)	425 (22.1 %)

from the results of the more rigorous proposed model. This accuracy limitation is particularly important in the design optimization problem, which was usually addressed in the literature using the assumption of uniform physical properties.

The flexibility and accuracy of the proposed model indicate that it can be an important resource for the development of a new class of design algorithms, departing from simplified analytical solutions toward more rigorous simulation tools. The adoption of an automatic solution for the design problem will be viable only if the practitioners rely on the accuracy of the model, which justifies the importance of the proposed approach.

Declaration of Competing Interest

The authors declare that they have no known competing financial interests or personal relationships that could have appeared to influence the work reported in this paper.

Data availability

Data will be made available on request.

Acknowledgments

André L. M. Nahes thanks the Brazilian National Agency for Petroleum, Natural Gas and Biofuels (ANP) and the Coordination for the Improvement of Higher Education Personnel (CAPES) for the scholarships. André L. H. Costa thanks the National Council for Scientific and Technological Development (CNPq) for the research productivity fellowship (Process 310390/2019-2) and the financial support of the Prociência Program (UERJ). Miguel Bagajewicz thanks the visiting researcher scholarship from UERJ (PAPD Program) for part of the time of the development of this work.

Appendix A. Supplementary data

Supplementary data to this article can be found online at https://doi.org/10.1016/j.applthermaleng.2022.119197.

References

[1] C. Bai, G. Zhang, Y. Qiu, X. Leng, M. Tian, A new method for heat transfer and fluid flow performance simulation of plate heat exchangers, Numer. Heat Transf. B: Fundam. 75 (2019) 93–110.
[2] E. Cao, Heat Transfer in Process Engineering, McGraw-Hill, New York, 2010.
[3] C. J. Mulanix Company, Inc. Replacement Plate Heat Exchanger Gaskets & Plates for GEA Products. https://www.cjmulanixco.com/Gea/index.php, **2022a**.
[4] C. J. Mulanix Company, Inc. Replacement Plate Heat Exchanger Gaskets & Plates for Alfa Laval Products. https://www.cjmulanixco.com/Alfa-Laval/index.php, **2022b**.
[5] S.C. Chapra, R.P. Canale, Numerical Methods for Engineers; McGraw-Hill, Higher Education (2008).
[6] H. Dardour, S. Mazouz, A. Bellagi, Numerical analysis of plate heat exchanger performance in co-current fluid flow configuration, Int. J. Mech. Ind. Aerosp. Sci. 3 (2009) 150–154.
[7] D. Dovic, I. Horvat, P. Filipovic, Impact of velocities and geometry on flow components and heat transfer in plate heat exchangers, Appl. Therm. Eng. 197 (2021) 117–371.
[8] T.M.A. Elmaaty, A.E. Kabeel, M. Mahgoub, Corrugated plate heat exchanger review, Renew. Sust. Energ. Rev. 70 (2017) 852–860.
[9] Z. Guo-Yan, W. En, T. Shan-Tung, Techno-economic study on compact heat exchangers, Int. J. Energy Res. 32 (2008) 1119–1127.
[10] J.A.W. Gut, J.M. Pinto, Modeling of plate heat exchangers with generalized configurations, Int. J. Heat Mass Transf. 42 (2003) 6112–6124.
[11] J.A.W. Gut, J.M. Pinto, Optimal configuration design for plate heat exchangers, Int. J. Heat Mass Transf. 47 (2004) 4833–4848.
[12] H. Hajabdollahi, M. Naderi, S. Adimi, A comparative study on the shell and tube and gasket-plate heat exchangers: The economic viewpoint, Appl. Therm. Eng. 92 (2016) 271–282.
[13] X. Han, L. Cui, S. Chen, G. Chen, Q. Wang, Numerical and experimental study of chevron, corrugated-plate heat exchangers, Int. Commun. Heat Mass Transf. 37 (2010) 1008–1014.
[14] M. Imran, N.A. Pambudi, M. Farooq, Thermal and hydraulic optimization of plate heat exchanger using multi objective genetic algorithm, Case Stud. Therm. Eng. 10 (2017) 570–578.
[15] F.P. Incropera, D.P. Dewitt, Fundamentals of heat and mass transfer, John Wiley & Sons, New York, 2007.
[16] M.A. Jamil, Z.U. Din, T.S. Goraya, H. Yaqoob, S.M. Zubair, Thermal-hydraulic characteristics of gasketed plate heat exchangers as a preheater for thermal desalination systems, Energy Convers. Manag. 205 (2020), 112425.
[17] M.A. Jamil, T.S. Goraya, H. Yaqoob, M.W. Shahzad, S.M. Zubair, Experimental and numerical analysis of a plate heat exchanger using variable heat transfer coefficient, Heat Transf. Eng. 43 (18) (2022) 1566–1578.
[18] S. Kakaç, H. Liu, Heat Exchangers: Selection, Rating, and Thermal Design, 2nd ed., CRC Press, Boca Raton, 2002, pp. 373–412.
[19] S.G. Kandlikar, R.K. Shah, Asymptotic effectiveness-NTU formulas for multipass plate heat exchangers, ASME J. Heat Transf. 111 (1989) 314–321.

[20] S.G. Kandlikar, R.K. Shah, 1989, Multipass plate heat exchangers—Effectiveness-NTU results and guidelines for selecting pass arrangements, ASME J. Heat Transf. 111 (1989) 300–313.
[21] S. Kumar, S.K. Singh, D. Sharma, A comprehensive review on thermal performance enhancement of plate heat exchanger, Int. J. Thermophys. 43 (2022) 109.
[22] K. Kurose, N. Watanabe, K. Miyata, H. Mori, Y. Hamamoto, S. Umezawa, Numerical simulation of flow and cooling heat transfer of supercritical pressure refrigerants in chevron-type plate heat exchanger, Int. J. Heat Mass Transf. 180 (2021), 121758.
[23] M. Lyytikäinen, T. Hämäläinen, J. Hämäläinen, Fast modelling tool for plate heat exchangers based on depth-averaged equations, Int. J. Heat Mass Transf. 52 (2009) 1132–1137.
[24] S. Mohebbi, F. Veysi, Numerical investigation of small plate heat exchangers performance having different surface profiles, Appl. Therm. Eng. 188 (2021), 116616.
[25] F.A.S. Mota, M.A.S.S. Ravagnani, E.P. Carvalho, Optimal design of plate heat exchangers, Appl. Therm. Eng. 63 (2014) 33–39.
[26] M. Picón-Núñez, G.T. Polley, D. Jantes-Jaramillo, Alternative design approach for plate and frame heat exchangers using parameter plots, Heat Transfer Eng. 31 (2010) 742–749.
[27] G.T. Polley, M.M. Abu-Khader, Compensating for End Effects in Plate and frame Heat Exchangers, Heat Transfer Eng. 10 (2005) 3–6.
[28] H. Qiao, V. Aute, H. Lee, K. Saleh, R. Radermacher, A new model for plate heat exchangers with generalized flow configurations and phase change, J. Int. Acad. Refrig. 36 (2013) 622–632.
[29] B.D. Raja, R.L. Jhala, V. Patel, Thermal-hydraulic optimization of plate heat exchanger: A multi-objective approach, Int. J. Therm. Sci. 124 (2018) 522–535.
[30] R.K. Shah, D.P. Sekulic, Fundamentals of Heat Exchanger Design, John Wiley & Sons, New York, 2003.
[31] E.A.D. Saunders, Heat Exchangers: Selection, Design, and Construction, John Wiley & Sons, New York, 1988.
[32] H. Shokouhmand, M. Hasanpour, Effect of flow maldistribution on the optimal design of plate heat exchanger using constrained multi objective genetic algorithm, Case Stud. Therm. Eng. 18 (2020), 100570.
[33] J.S.R. Tabares, L. Perdomo-Hurtado, J.L. Aragón, Study of gasketed-plate heat exchanger performance based on energy efficiency indexes, Appl. Therm. Eng. 159 (2019), 113902.
[34] A. Yildiz, M.A. Ersöz, Theoretical and experimental thermodynamic analyses of a chevron type heat exchanger, Renew. Sust. Energ. Rev. 42 (2015) 240–253.
[35] W. Yoon, J.H. Jeong, Development of a numerical analysis model using a flow network for a plate heat exchanger with consideration of the flow distribution, Int. J. Heat Mass Transf. 112 (2017) 1–17.
[36] K. Xu, K. Qin, W. Wu, R. Smith, A new computer-aided optimization-based method for the design of single multi-pass plate heat exchangers, Processes. 10 (2022) 767.
[37] J. Zhu, W. Zhang, Optimization design of plate heat exchangers (PHE) for geothermal district heating systems, Geothermics. 33 (2004) 337–347.